CHAPTER V

Thermodynamics of Ionic Association of Tetraphenylphosphonium, Tetraphenylarsonium, and Some Common Cations in 2-Methoxyethanol using Conductometry and FT-Raman Spectroscopy

With the development of the laser, the era of routine laser-Raman spectroscopic work has truly arrived, eliminating many problems of sample decomposition. The Fourier Transform (FT) technique brings to the recording of Raman spectra many advantages like, wavenumber accuracy, spectra summation and subtraction, short measurement times, etc. State-of- the-art FT laser-Raman spectrometers use a Nd-YAG laser operating at 1064 nm, which minimizes the troublesome fluorescence.[1]

FTIR and FT Raman techniques are very much complementary. In a dual instrument, in which switching between the FTIR and FT Raman modes is carried out by computer, both IR and Raman spectra can be obtained easily and speedily on the same sample. The principal advantages of laser-Raman spectroscopy over infrared are its increased sensitivity, the ease of sample preparation and the fact that water makes an ideal solvent.

The Raman effect depends on the polarizability of a vibrating group in a molecule, and on its ability to interact and couple with an exciting radiation whose frequency does not match that of the vibration itself. Many absorptions that are weak in infrared give strong absorptions in Raman spectra. Due to these various advantages we employed FT Raman spectroscopy for our investigation.

As the second part of our comprehensive programme to study the solvation and association behaviour of some electrolytes in different non-aqueous solvents from the measurements of various transport, thermodynamic, and spectroscopic properties,[2-4] we attempted to unravel the nature of various types of interactions prevailing in solutions of tetraphenylarsonium chloride (Ph_4AsCl), tetraphenylphosphonium chloride(Ph_4PCl), tetraphenylphosphonium bromide (Ph_4PBr), lithium tetrafluoroborate ($LiBF_4$), and sodium tetrafluoroborate ($NaBF_4$) in 2-methoxyethanol (ME). As it is a monomethyl ether of ethylene glycol, it is very likely to show physicochemical properties midway between protic and aprotic solvents. Hence, it is of much interest to study the behavior of electrolytes in such a solvent medium.

In this chapter we present our precise measurements of electrical conductances and Fourier Transform(FT)-Raman spectra of solutions of tetraphenylarsonium chloride (Ph_4AsCl), tetraphenylphosphonium chloride(Ph_4PCl), tetraphenylphosphonium bromide (Ph_4PBr), lithium tetrafluoroborate ($LiBF_4$), and sodium tetrafluoroborate ($NaBF_4$) in 2-methoxyethanol (ME) at temperatures $288.15 \leq T/K \leq 308.15$. The conductance data were analyzed by the 1978 Fuoss conductance-concentration equation. Thermodynamics of the association processes have also been studied.

5.1 EXPERIMENTAL SECTION

5.1.1 Materials:

2-Methoxyethanol (G.R. E Merck) was purified as reported in Chapter 3 and having a density of 0.96002 g cm^{-3}, a coefficient of viscosity of 1.5414 mPa.s, and a

specific conductance of *ca.* 1.01 x 10^{-6} S cm^{-1} at 298.15 K. The salts were prepared and also purified as described in Chapter 3.

5.1.2 Apparatus and Procedures:

Conductance measurements were carried out on a pye-Unicam PW 9509 conductivity meter and the details of the experimental procedure have been described earlier. Solutions were prepared by mass for the conductance runs, the molalities being converted to molarities by the use of densities measured with an Ostwald-Sprengel type pycnometer of about 25 cm^3 capacity. Several independent solutions were prepared and runs were performed to ensure the reproducibility of the results. Due correction was made for the specific conductance of the solvent at all temperatures.

FT-Raman spectra were excited at 1064 nm using Nd:YAG laser and a Brucker IFS 66V optical bench with an FRA 106 Raman module attached to it. Laser power was set at 200 mW, and 250 (averaged) scans were accumulated with a resolution of 2 cm^{-1}. The spectra were recorded by the Regional Sophisticated Instrumentation Centre, Indian Institute of Technology, Madras. The dielectric constants of 2-methoxyethanol at different temperatures were taken from Table I, in Chapter 4.

5.2 RESULTS

5.2.1 Conductance:

The measured molar conductances (Λ) of electrolyte solutions as a function of molar concentration (c) at 288.15, 293.15, 298.15, and 308.15 K are given in Table 1. The conductance data have been analyzed by the 1978 Fuoss conductance-concentration equation.[5,6] For a given set of conductivity values ($c_j, \Lambda_j; j = 1,...,n$), three adjustable parameters, the limiting molar conductivity (Λ^0), association constant (K_A), and the cosphere diameter (R), are derived from the following set of equations:

$$\Lambda = p[\Lambda^0(1+R_X)+E_L] \tag{1}$$

$$p = 1-\alpha(1-\gamma) \tag{2}$$

$$\gamma = 1-K_A c\gamma^2 f^2 \tag{3}$$

$$-\ln f = \beta k / 2(1+kR) \tag{4}$$

$$\beta = e^2 / Dk_B T \tag{5}$$

$$K_A = K_R / (1-\alpha) = K_R(1+K_S) \tag{6}$$

where the symbols have their usual significance. The computations were performed on a computer using the programme suggested by Fuoss. The initial Λ^0 values for the iteration procedure were obtained from Shedlovsky extrapolation[7] of the data. Input for the program is the set $(c_j, \Lambda_j; j = 1,...,n), n, D, \eta, T$, initial value of Λ^0, and an instruction to cover a preselected range of R values.

In practice calculations are made by finding the values of Λ^0 and α which minimize the standard deviation, σ,

$$\sigma^2 = \sum[\Lambda_j(calcd) - \Lambda_j(obsd)]^2 / (n-2) \quad (7)$$

for a sequence of R values and then plotting σ against R; the best-fit R corresponds to the minimum in σ vs R curve. However, since a rough scan using unit increment of R values from 4 to 20 gave no significant minima in the σ(%) vs R curves, the R value was assumed to be $R = a + d$, where a is the sum of the ionic crystallographic radii and d is given by[6]

$$d = 1.183(M / \rho_0)^{1/3} \quad (8)$$

where M is the molecular weight of the solvent and ρ_0 its density.

The values of Λ^0, K_A, and R obtained by this procedure are reported in Table 2.

5.2.2 FT-Raman Spectra:

The Raman spectra of pure 2-methoxyethanol and of the solutions of Ph_4AsCl, Ph_4PCl, Ph_4PBr, $LiBF_4$, and $NaBF_4$ in 2-methoxyethanol in the range 3500 - 100 cm^{-1} have been presented in Figures 1 to 5. The principal bands observed have been listed in Table 3.

5.3 DISCUSSION

5.3.1 Limiting Molar Conductance and Association Constant:

Table 2 shows that for all salts the limiting molar conductances (Λ^0) increase as the temperature increases. The Λ^0 values have been fitted to the following polynomial:

$$\Lambda^0 = a_0 + a_1(298.15 - T) + a_2(298.15 - T)^2 \quad (9)$$

and the coefficients of these fits are given in Table 4 together with the standard percentage errors ($\sigma\%$).

The single-ion conductivities at different temperatures have been calculated from the reference electrolyte Bu_4NBPh_4.[8] The single-ion conductivities ($\lambda^0_\pm$) along with the Walden products ($\lambda^0_\pm \eta_0$) are reported in Table 5.

The single-ion conductivities have also been fitted to the following polynomial equation:

$$\lambda^0_\pm = b_0 + b_1(298.15 - T) + b_2(298.15 - T)^2 \quad (10)$$

and the coefficients of the fits along with the $\sigma\%$ values are recorded in Table 6.

All these electrolytes are found to be moderately associated (*cf.* K_A values from Table 2) in 2- methoxyethanol at all the temperatures investigated. These electrolyte solutions, in general, show small negative temperature dependence of K_A, which is a

quite normal behaviour for molecular ions with non-electrostatic contributions to the inter-ionic potential, also known for acetate, and fluoroacetate salts in dimethylsulfoxide[9] and tetraalkylammonium salts in acetonitrile[10] and methanol.[11]

5.3.2 Thermodynamics of Ion-Pair Formation:

The standard Gibbs energy changes for the ion association process, ΔG^0, can be calculated from the association constants using the equation:

$$\Delta G^0 = -RT \ln K_A \tag{11}$$

In order to evaluate the standard enthalpy change, ΔH^0, and the standard entropy change, ΔS^0, we have fitted the ΔG^0 values to a polynomial of T of the type:

$$\Delta G^0 = c_0 + c_1(298.15 - T) + c_2(298.15 - T)^2 \tag{12}$$

and the coefficients of the fits are compiled in Table 7, together with the $\sigma\%$ values of the fits.

The ΔH^0, and ΔS^0 values of the ion-association process can then be evaluated from the temperature dependence of ΔG^0 values as follows:

$$\Delta H^0 = -T^2 \left[\frac{d(\Delta G^0 / T)}{dT} \right]_p \tag{13}$$

$$\Delta S^0 = -\left(\frac{d\Delta G^0}{dT}\right)_p \tag{14}$$

The standard values of the thermodynamic parameters at 298.15 K can, therefore, be expressed as:

$$\Delta G^0_{298.15} = c_0 \tag{15}$$

$$\Delta S^0_{298.15} = c_1 \tag{16}$$

$$\Delta H^0_{298.15} = c_0 + 298.15 c_1 \tag{17}$$

It is observed from Table 7 that the ΔS^0 values of ion association for all these electrolytes ($LiBF_4$ being an exception) are positive. These positive ΔS^0 values may be attributed to the increasing number of degrees of freedom after association mainly due to the release of solvent molecules as shown below

$$M^+.n(ME) + X^-.m(ME) = MX.z(ME) + (n+m-z)ME \tag{18}$$

In other words, the solvation of the individual ions is weakened as soon as these ion pairs are formed. A decrease in the entropy for $LiBF_4$ solution, on the other hand, suggests that the ion pairs that are formed organize the solvent molecules in their vicinity better than the ions.

It is especially noteworthy that the ΔH^0 values for all the electrolytes are negative.

The electrostatic theories of ionic association,[12] however, never give negative values for ΔH^0, since the theoretical equation for ΔH^0 contains the $\left[1+\left(\frac{d\ln D}{d\ln T}\right)_p\right]$ term; thus the experimental value of $\left(\frac{d\ln D}{d\ln T}\right)_p$ makes the theoretical ΔH^0 value positive, contrary to expectation.

The negative values of ΔH^0 can be explained by considering the participation of specific covalent interaction in the ion association process. Here, the covalent interaction somewhat works between the ions and hence, the binding enthalpy between the ions is sufficiently negative to compensate for the positive contribution from the weakening of ion solvation. Consequently, ΔG^0 of the ion association should have a large negative value (a large K_A value) and should depend on the kind of ions and this is found to be true here.

The non-Coulombic contribution to the Gibbs energy, ΔG^*, has been calculated from the following equation[9]

$$\Delta G^* = N_A W_{\pm}^* \tag{19}$$

$$K_A = (4\pi N_A / 1000)\int_a^R r^2 \exp\left(\frac{2q}{r} - \frac{W_{\pm}^*}{kT}\right)dr \tag{20}$$

where the symbols have their usual meaning. The quantity 2q/r is the Coulombic part of the interionic mean force potential and $W_{\pm}^*$ is its non-Coulombic part.

The procedure for the evaluation of the non-Coulombic contribution to the entropy and enthalpy (ΔS^* and ΔH^* respectively) is similar to that used for obtaining ΔS^0 and ΔH^0.

The ΔG^* values at different temperatures were fitted to the polynomial:

$$\Delta G^* = c_0^* + c_1^*(298.15 - T) + c_2^*(298.15 - T)^2 \tag{21}$$

and the coefficients of the fits along with the $\sigma\%$ values are given in Table 8.

The values of $\Delta G^*, \Delta S^*$, and ΔH^* at 298.15 K are then easily obtained from the following equations:

$$\Delta G^*_{298.15} = c_0^* \tag{22}$$

$$\Delta S^*_{298.15} = c_1^* \tag{23}$$

$$\Delta H^*_{298.15} = c_0^* + 298.15 c_1^* \tag{24}$$

The non-Coulombic parts of the Gibbs energy, $\Delta G^*_{298.15}$, of all the salts are found to be small (Table 8) - 19% (Ph_4AsCl), 19% (Ph_4PCl), 24% (Ph_4PBr), 23%($LiBF_4$), and 20% ($NaBF_4$) in 2-methoxyethanol. This indicates that the Coulombic forces play a major role in the association processes. This is further supported by the fairly higher values of the Coulombic parts of ΔS^0 and ΔH^0 in comparison with their non-Coulombic counterparts.

5.3.3 Raman Spectral Behaviour:

Partial band assignments for the pure solvent as well as for the electrolyte solutions have been made and discussed accordingly. From Figures 1 through 5 we see that 2-methoxyethanol (ME) shows $\nu_s(C-O)$ in the range 800 - 900 cm^{-1}, and $\nu_s(O-H)$ in the range 100 - 1100 cm^{-1}. The CH_3-O symmetric and asymmetric bending vibrations of ME appear as a closely spaced doublet at 1457 and 1471 cm^{-1} respectively. The solvent also exhibits its stretching modes in the wavenumber range 2800 - 2950 cm^{-1}. It can be seen from Table 3 that the spectra of the salt solutions show several remarkable changes from that of the pure solvent. For $LiBF_4$ solution, three new bands of medium intensity appear in the range 375 - 550 cm^{-1}. These bands may be assigned to the vibration primarily involving the lithium ion. Similar types of bands in this frequency range have also been observed in 1,2-dimethoxyethane solutions.[3] The sodium ion in $NaBF_4$ also exhibits similar bands, however, with very low intensity.

Phosphorus and arsenic atoms present in tetraphenylphosphonium and tetraphenylarsonium ions respectively show Raman peaks at 254 and 238 cm^{-1} respectively in this lower frequency range.

From the spectra we see that $LiBF_4$ and $NaBF_4$ solutions of 2-methoxyethanol show new bands with maxima around 700 cm^{-1}. The strong bands at 1587 cm^{-1} for Ph_4PBr and at 1581 cm^{-1} for Ph_4AsCl solutions are also observed in their Raman spectra. The appearance of these new bands for these salts has been assigned to the

"spectroscopically free" anion X^- ($X = BF_4, Cl, Br$) in 2-methoxyethanol, i.e., to the solvent-separated ion-pair M^+SX^- (S is the solvent molecule) and/or to the solvent-separated dimer $M^+SX^- \ldots M^+SX^-$, spectroscopically indistinguishable from each other.

The above observations can be interpreted in terms of the following eigen multistep mechanism:

$$M^+ + X^- = M^+SX^- = MX \tag{25}$$

$$2M^+SX^- = M^+SX^- \ldots M^+SX^- \tag{26}$$

$$2MX = (MX)_2 \tag{27}$$

Thus, for these electrolytes, one would expect the presence of an equilibrium between the solvent-separated and contact ion pairs as represented by eq 25 which is strongly shifted towards the left due to the presence of "spectroscopically free" anions. The equilibrium represented by eq 26 to form the solvent-separated dimer may also exist since M^+SX^- and $M^+SX^- \ldots M^+SX^-$ are indistinguishable from each other by Raman spectra. However, no contact quadrupole is expected to form through eq 27 for the electrolytes for the reasons just mentioned above. This also supports the moderate association of these salts as manifested by the conductivity study.

The complexation of 2-methoxyethanol with the cations has been manifested by the shifts of the Raman band of the symmetric $C-O$ stretching mode as well as that of the symmetric $O-H$ mode of pure solvent. The $\nu_s(C-O)$ band of 2-methoxyethanol in salt

solutions shifts slightly from the corresponding peak in pure 2-methoxyethanol. This indicates the coordination of the lithium, sodium, tetraphenylphosphonium, and tetraphenylarsonium ions with the oxygen atoms of 2-methoxyethanol molecules. But, the shifts are too small to draw any definitive conclusion as to which of the two oxygen atoms in 2-methoxyethanol molecules get coordinated with the cations. This is, however, nicely demonstrated by the sizeable shifts of $\nu_s(O-H)$ bands in the electrolyte solutions compared to shifts in the solvent $\nu_s(O-H)$ peak. The $\nu_s(O-H)$ peak appears at 1074.6 cm^{-1} in pure 2-methoxyethanol, and those in all the salt solutions shift to the shorter wavenumber region. The probability of complexation of the cations with 2-methoxyethanol molecules through the $-OCH_3$ group (with higher electron density on the oxygen atom arising due to the electron repelling inductive effect of CH_3 group than on the alcoholic oxygen atom) makes the $-OH$ moiety rather free, and in this case the band shifts to the shorter wavenumber region. In case of linkage through the $-OH$ group, the reverse trend should have been observed. The red-shift of the $\nu_s(O-H)$ band in solutions amply indicates the complexation through the ethereal oxygen atom.

In the higher wavenumber region, the pure solvent shows three peaks at 2829.7, 2890.3 and 2942.4 cm^{-1}. The peak at 2829•7 cm^{-1} may be assigned to the $C-O-C$ symmetric stretching and that at 2942.4 cm^{-1} may be assigned to the $C-O-H$ symmetric stretching of 2-methoxyethanol. The peak of medium intensity at 2890.3 cm^{-1} appears due to the intramolecular hydrogen-bonding of alcoholic hydrogen with the ethereal oxygen atom. For the alkali metal salts it is observed that all these three peaks appear at higher wavenumbers in the spectra. As a result of coordination of alkali metal ions with the lone

pair of electrons on the ethereal oxygen atom, the lone pairs get shifted to the alkali cations, thus increasing the stretching frequency of the $C-O-C$ mode in salt solutions. Due to this displacement of the lone pairs towards the alkali metal ions, the intramolecular hydrogen bonding will be weaker which results in a shift of both the $C-O-H$ symmetric stretching mode and the $O-H\cdots O$ band to longer wavenumbers. The shifting of the $C-O-C$ and $O-H\cdots O$ bands is found to be in the order $LiBF_4 > NaBF_4$. This may be ascribed to the greater displacement of the ethereal oxygen lone pair towards the lithium ion with higher surface charge density compared to the sodium ion. The anomalous order in shifting of the $C-O-H$ bands might possibly be due to the greater interaction of the sodium ion with 2-methoxyethanol molecules as demonstrated conductometrically.

For Ph_4PBr and Ph_4AsCl solutions, the $C-O-C$ and $C-O-H$ bands of pure 2-methoxyethanol shift towards the shorter wavenumbers, while the $O-H\cdots O$ band exhibits a blue shift. Both the larger tetraphenylphosphonium and tetraphenylarsonium ions coordinate with the ethereal oxygen atom, though the strength of coordination is sufficiently weaker compared to the alkali metal ions because of the larger size and smaller charge density of these cations. Thus the $C-O-C$ and $C-O-H$ bands of pure 2-methoxyethanol should not shift to the higher wavenumber regions like the alkali metal ions in these cases. A possible explanation may be that though the electron pairs of the ethereal oxygen atom coordinate with these cations (the extent of displacement of lone pairs is small enough compared to the alkali cations), but their bulky sizes hinder the $C-O-C$ and $C-O-H$ stretching vibrations, resulting in red shifts for these bands in

salt solutions. The shift of the $O-H$- - -O bands to the longer wavenumbers may be ascribed to the loosening of the intramolecular hydrogen bonding arising out of this coordination.

The four $P-Ph$ σ-bonds are sp^3 hybridised. The phenyl groups show a strong peak at the 3060 cm^{-1} region. As the phosphorus atom has a positive charge, the vacant 3d orbitals are compact and in shape to participate in bonding as acceptor of electrons, the ethereal oxygen atom lone pairs being the donors. The d-orbitals in phosphorus are usually diffuse. But when phosphorus consists of a positive charge and its ligands are electronegative, its five vacant d-orbitals are compact and in shape to accept electrons - in this case from the ethereal oxygen atom lone pairs. In the case of tetraphenylarsonium ions, due to the larger size of the arsenic atom, they will be less compact than the tetraphenylphosphonium ions and so coordination through lone pairs will be easier. This is manifested by the spectral shifts. As the arsenic atom appears to be more metallic in nature than phosphorus, the tetraphenylarsonium ion pulls the ethereal oxygen lone pair more effectively towards it, causing greater loosening of the intramolecular hydrogen-bonding; thus the shift of the $O-H$---O bands will be higher with tetraphenylarsonium ions than with tetraphenylphosphonium ions. For the other bands, e.g., $C-O-C$ and $C-O-H$ vibrations, the red shiftings are found to be in the order: tetraphenylphosphonium ion > tetraphenylarsonium ion. Thus lower shifting with tetraphenylarsonium ion may be due to the greater size of the tetraphenylarsonium ion which makes free movement of $C-O-C$ and $C-O-H$ bands quite restricted.

It may thus be concluded that all these electrolytes remain strongly associated in 2-methoxyethanol to form ion pairs and the solvation of the ions is weakened as soon as the ion pair is formed. The results indicate that the Coulombic forces play a major role in the association process. All these electrolytes are found to exist in ME solution as solvent-separated ion pairs and/or solvent-separated dimers, thus exhibiting a very intense peak for the "spectroscopically free" anion. Moreover, the chelation of ME with the cations is taking place through the lone pairs of electrons on the ethereal oxygen atom.

References

1. W. Kemp, *Organic Spectroscopy*, 3rd (ELBS) ed., Macmillan Press, Hampshire, U.K., 1993, pp. 95-97.
2. B. Das and D. K. Hazra, *J. Phys. Chem.*, **99**, 269, 1995.
3. P. K. Muhuri, B. Das and D. K. Hazra, *J. Phys. Chem.B.*, **101**, 3329, 1997.
4. P. J. Victor, P. K Muhuri, B. Das and D. K. Hazra, *J. Phys. Chem.B.*, **103**, 11227, 1999.
5. R. M. Fuoss, *Proc. Natl. Acad. Sci. U.S.A.*, **75**, 16, 1978.
6. R. M. Fuoss, *J. Phys. Chem.*, **82**, 2427, 1978.
7. R. M. Fuoss and T. Shedlovsky, *J. Am. Chem. Soc.*, **71**, 1496, 1949.
8. B. Das and D. K. Hazra, *Bull. Chem. Soc. Jpn.*, **68**, 734, 1995.
9. J. Barthel, H. J. Gores and L. Kraml, *J. Phys. Chem.*, **100**, 1283, 1996.
10. J. Barthel, L. Iberl, J. Rossmaier, H. J. Gores and B. Kaukal, *J. Soln. Chem.*, **19**, 321, 1990.
11. J. Barthel, M. Krell, L. Iberl and F. Feuerlein, *J. Electroanal. Chem.*, **214**, 485, 1986.
12. R. M. Fuoss, *J. Am. Chem. Soc.*, **80**, 5059, 1958.

TABLE 1: Molar Conductivities of Electrolytes in 2-Methoxyethanol at 288.15, 293.15, 298.15, and 308.15 K

T = 288.15 K		T = 293.15 K		T = 298.15 K		T = 308.15 K	
$c \times 10^4$/ mol dm^{-3}	Λ / S cm^2 mol^{-1}	$c \times 10^4$/ mol dm^{-3}	Λ / S cm^2 mol^{-1}	$c \times 10^4$/ mol dm^{-3}	Λ / S cm^2 mol^{-1}	$c \times 10^4$/ mol dm^{-3}	Λ / S cm^2 mol^{-1}
			Ph_4AsCl				
6.5187	23.54	4.2025	26.87	4.0000	29.52	3.8416	34.47
7.5372	23.21	5.1756	26.44	5.0625	29.01	5.0176	33.87
8.5558	22.91	6.0530	26.08	6.2413	28.52	5.9524	33.44
9.5743	22.65	7.0618	25.73	7.0195	28.22	7.0602	32.96
10.5929	22.39	8.0034	25.39	8.0620	27.84	8.0015	32.60
11.0003	22.27	9.0123	25.07	9.4899	27.38	9.0101	32.23
12.0188	22.01	10.0211	24.74	10.4250	27.05	10.0187	31.87
13.0374	21.79	11.0299	24.46	11.4675	26.73	11.0273	31.55
14.0559	21.56	12.0388	24.18	12.4405	26.40	12.0359	31.22
			Ph_4PCl				
5.0625	24.35	3.4596	27.54	5.2900	29.09	3.0276	35.00
6.0784	23.97	4.6447	26.95	6.8270	28.48	3.6100	34.63
7.0071	23.64	6.0520	26.36	7.8151	28.12	5.0842	33.81
8.0201	23.33	6.9999	25.98	8.8033	27.79	6.5459	33.09
9.0332	23.01	8.0208	25.62	9.7914	27.50	7.5628	32.65
10.0463	22.70	9.1145	25.24	10.7795	27.23	8.5161	32.26
11.0594	22.44	10.0624	24.94	11.7676	26.95	9.5329	31.87
12.0724	22.17	11.0103	24.65	12.7557	26.67	10.5497	31.49
13.5076	21.81	12.0639	24.34	13.7439	26.44	11.5030	31.18

(Table 1 Continued)

(Table 1 Continued)

Ph_4PBr

2.1408	29.14	4.6656	29.76	2.0991	34.36	2.1377	40.70
3.1743	28.38	5,6644	29.22	3.1825	33.46	3.1437	39.74
4.2077	27.74	6.5487	28.79	4.1982	32.71	4.2125	38.86
5.2412	27.17	7.5053	28.36	5.2816	32.04	5.2185	38.14
6.2747	26.69	8.5354	27.93	6.2973	31.47	6.2873	37.41
7.3082	26.20	9.5656	27.51	7.3130	30.95	7.3562	36.79
8.4155	25.73	10.5221	27.16	8.3965	30.41	8.3622	36.24
9.4490	25.35	10.5522	26.77	9.4122	29.95	9.4310	35.67
10.4824	24.92	12.5088	26.43	10.4956	29.48	10.4370	35.17

$LiBF_4$

4.4944	30.22	4.2436	33.10	4.1616	35.30	4.1616	40.34
5.5697	29.58	5.0271	32.58	5.0544	34.71	5.0667	39.72
6.0540	29.30	6.0261	31.97	6.0067	34.14	6.0213	39.13
7.0226	28.80	7.0231	31.43	7.0322	33.56	7.0493	38.51
8.0720	28.29	8.0581	30.89	8.0577	33.02	8.0039	38.01
9.0406	27.84	9.0192	30.44	9.0100	32.56	9.0319	37.48
10.0092	27.42	10.0542	29.97	9.9623	32.10	10.0599	37.02
11.0586	26.98	11.0153	29.54	11.0611	31.63	11.0145	36.58
12.0272	26.59	12.0502	29.13	12.0134	31.20	12.0425	36.14

$NaBF_4$

1.0250	30.94	1.0250	32.62	5.6644	31.53	2.0437	38.47
2.0505	29.92	2.0505	31.58	6.5832	31.10	3.0655	37.58
3.0785	29.17	3.0758	30.79	7.5237	30.70	4.0088	36.88
4.0222	28.59	4.0222	30.16	8.5817	30.28	5.0306	36.24
5.0475	28.00	5.0475	29.54	9.5222	29.93	6.0525	35.61
6.0727	27.53	6.0727	29.04	10.5802	29.54	7.0743	35.04
7.0980	27.06	7.0980	28.55	11.5207	29.21	8.0175	34.58
8.0444	26.60	8.0444	28.05	12.5787	28.85	9.0394	34.07
9.0697	26.25	9.0697	27.67	13.5191	28.56	10.2184	33.54
10.2527	25.77	10.2527	27.20				

TABLE 2: Conductance Parameters of Electrolytes in 2-Methoxyethanol at 288.15, 293.15, 298.15, and 308.15 K

electrolyte	T/K	Λ^0 / S cm^2 mol^{-1}	K_A / dm^3 mol^{-1}	R / $\overset{0}{A}$	σ%
Ph_4AsCl	288.15	28.33 ± 0.07	254 ± 6	10.91	0.08
	293.15	31.08 ± 0.06	246 ± 6	10.91	0.10
	298.15	33.98 ± 0.10	233 ± 9	10.92	0.16
	308.15	39.26 ± 0.07	186 ± 5	10.93	0.10
Ph_4PCl	288.15	28.78 ± 0.07	274 ± 7	10.81	0.11
	293.15	31.47 ± 0.07	257 ± 7	10.81	0.13
	298.15	34.03 ± 0.05	213 ± 4	10.82	0.06
	308.15	39.41 ± 0.07	208 ± 5	10.83	0.12
Ph_4PBr	288.15	32.48 ± 0.07	336 ± 9	10.97	0.17
	293.15	35.36 ± 0.10	340 ± 9	10.97	0.12
	298.15	38.25 ± 0.08	317 ± 8	10.98	0.16
	308.15	45.31 ± 0.09	297 ± 8	10.99	0.15
$LiBF_4$	288.15	36.26 ± 0.12	388 ± 12	7.70	0.13
	293.15	39.21 ± 0.11	350 ± 9	7.70	0.12
	298.15	41.52 ± 0.13	313 ± 10	7.71	0.14
	308.15	46.86 ± 0.09	224 ± 6	7.72	0.10
$NaBF_4$	288.15	33.07 ± 0.06	280 ± 7	8.26	0.18
	293.15	34.93 ± 0.07	276 ± 7	8.26	0.19
	298.15	37.66 ± 0.10	253 ± 8	8.27	0.11
	308.15	42.54 ± 0.09	228 ± 8	8.28	0.17

TABLE 3: Raman Frequencies in cm^{-1}[a]

ME	*Ph_4AsCl*	*Ph_4PBr*	*$LiBF_4$*	*$NaBF_4$*
-	238.1(m)	253.8(m)	-	-
-	-	-	376.8(m)	375.3(w)
-	-	-	425.8(m)	427.7(w)
-	-	-	541.5(m)	542.7(w)
-	-	-	766.4(m)	770.2(w)
834.7(s)	833.1(m)	832.9(s)	833.7(s)	834.5(s)
891.4(m)	894.6(w)	892.2(w)	892.6(m)	889.5(m)
1019.4(w)	1001.9(vs)	1001.3(s)	-	-
1074.6(w)	1023.6(m)	1027.3(m)	1065.4(m)	1069.0(w)
1457.0(s)	sh	1455.8(s)	1457.9(s)	1454.1(s)
1470.6(s)	1463.5(s)	1470.0(s)	sh	sh
-	1580.6(s)	1586.6(s)	-	-
2829.7(vs)	2828.4(s)	2829.1(m)	2835.5(vs)	2832.8(vs)
2890.3(m)	2896.5(m)	2891.0(m)	2895.1(m)	2892.1(m)
2942.4(s)	2937.0(s)	2923.1(s)	2943.5(s)	2944.8(s)
-	3063.0(vs)	3065.8(s)		

[a] sh = shoulder, w = weak, m = medium, s = strong, vs = very strong.

TABLE 4: Coefficients of the Polynomial, Equation 9.

electrolyte	a_0	a_1	a_2	σ %
Ph_4AsCl	33.93	-0.5481	-0.0015	0.066
Ph_4PCl	34.07	-0.5302	-0.0003	0.055
Ph_4PBr	38.32	-0.6390	0.0058	0.089
$LiBF_4$	41.67	-0.5236	-0.0010	0.162
$NaBF_4$	37.49	-0.4792	0.0029	0.209

TABLE 5: Limiting Ionic Conductances ($\lambda^0_\pm$/S cm^2 mol^{-1}) and Ionic Walden Products $\lambda^0_\pm\eta_0$/S cm^2 mol^{-1} Pa s) in 2-Methoxyethanol at 288.15, 293.15, 298.15, and 308.15 K

	288.15 K		293.15 K		298.15 K		308.15 K	
ion	$\lambda^0_\pm$	$\lambda^0_\pm\eta_0$	$\lambda^0_\pm$	$\lambda^0_\pm\eta_0$	$\lambda^0_\pm$	$\lambda^0_\pm\eta_0$	$\lambda^0_\pm$	$\lambda^0_\pm\eta_0$
Ph_4As^+	9.83	0.019	10.21	0.018	11.16	0.017	13.85	0.017
Ph_4P^+	10.28	0.020	10.60	0.018	11.21	0.017	14.00	0.018
Cl^-	18.50	0.036	20.87	0.036	22.82	0.035	25.41	0.032
Br^-	22.20	0.043	24.76	0.043	27.04	0.042	31.31	0.039

TABLE 6: Coefficients of the Polynomial, Equation 10.

ion	b_0	b_1	b_2	σ%
Ph_4As^+	11.11	-0.2026	0.00721	0.204
Ph_4P^+	11.25	-0.1847	0.00898	0.158
Cl^-	22.82	-0.3455	-0.00866	0.002
Br^-	27.07	-0.4544	-0.00313	0.059

TABLE 7: Coefficients of the Polynomial, Equation 12, and Thermodynamic Standard Data of the Association

electrolyte	c_0 $\Delta G^0_{298.15}$ / J mol^{-1}	c_1 $\Delta S^0_{298.15}$ / J K^{-1} mol^{-1}	$10^2\ c_2$ / J K^{-2} mol^{-1}	σ%	$c_0 + 298.15c_1$ $\Delta H^0_{298.15}$ / J mol^{-1}
Ph_4AsCl	-13504.9	6.38	178.80	0.025	-11602.7
Ph_4PCl	-13387.1	8.11	-190.62	0.316	-10969.1
Ph_4PBr	-14318.2	31.14	48.99	0.131	-5033.8
$LiBF_4$	-14241.4	-11.88	-80.44	0.009	-17783.4
$NaBF_4$	-13754.7	19.26	43.38	0.121	-8012.3

TABLE 8: Coefficients of the Polynomial, Equation 21, for the Non-Coulombic Contribution to the Association Process

electrolyte	c_0^* $\Delta G^*_{298.15}$ / J mol^{-1}	c_1^* $\Delta S^*_{298.15}$ / J K^{-1} mol^{-1}	$10^2\ c_2^*$ J K^{-2} mol^{-1}	σ%	$c_0^* + 298.15 c_1^*$ $\Delta H^*_{298.15}$ / J mol^{-1}
Ph_4AsCl	-2616.2	-41.29	182.33	0.094	-14926.8
Ph_4PCl	-2496.5	-39.49	-182.95	1.578	-14270.4
Ph_4PBr	-3437.0	-16.47	56.72	0.531	-8347.5
$LiBF_4$	-3255.2	-59.38	87.96	0.037	-20959.3
$NaBF_4$	-2776.3	-28.15	50.90	0.578	-11199.0

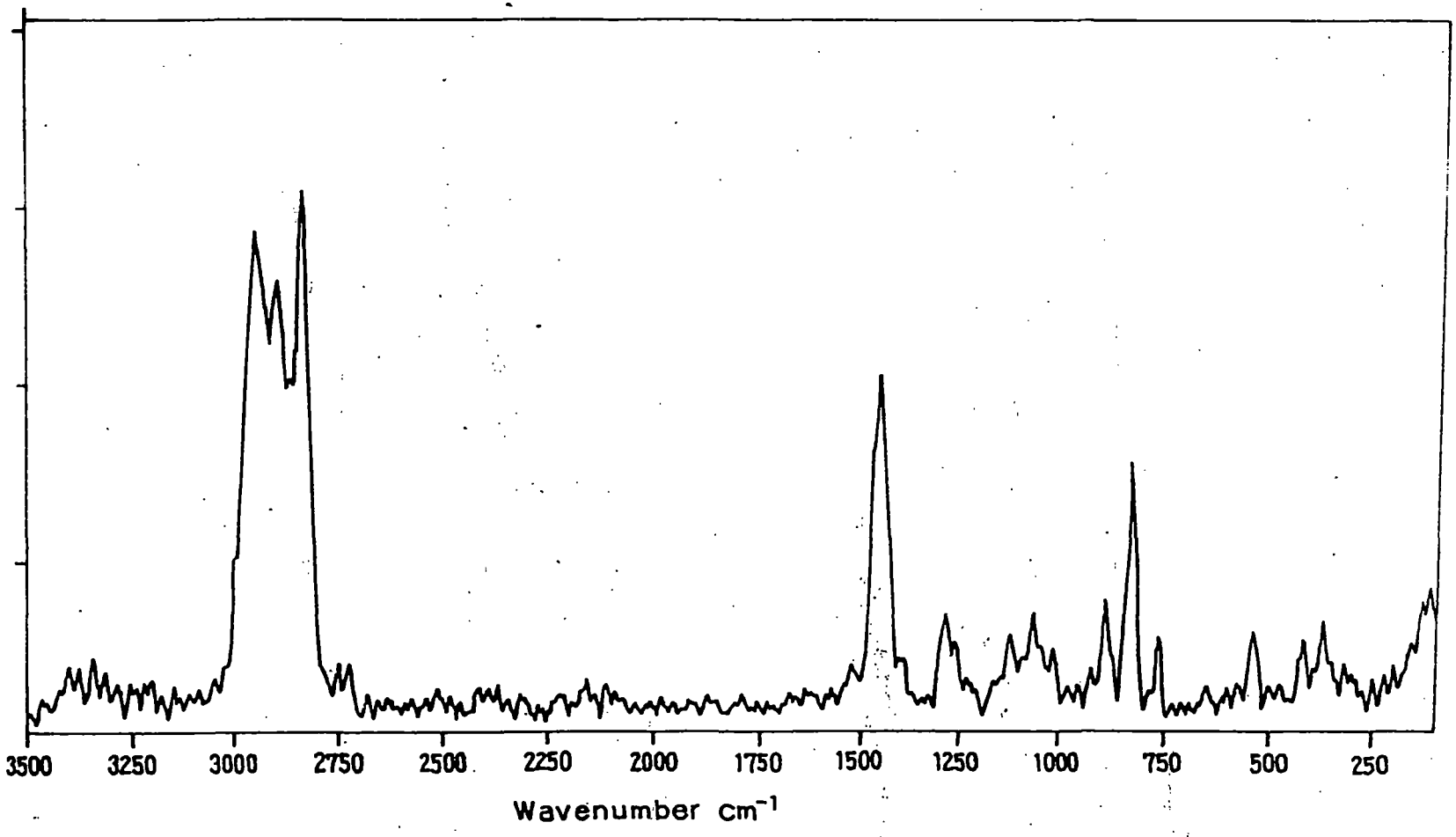

Figure 1: FT-Raman spectrum of 2-methoxyethanol.

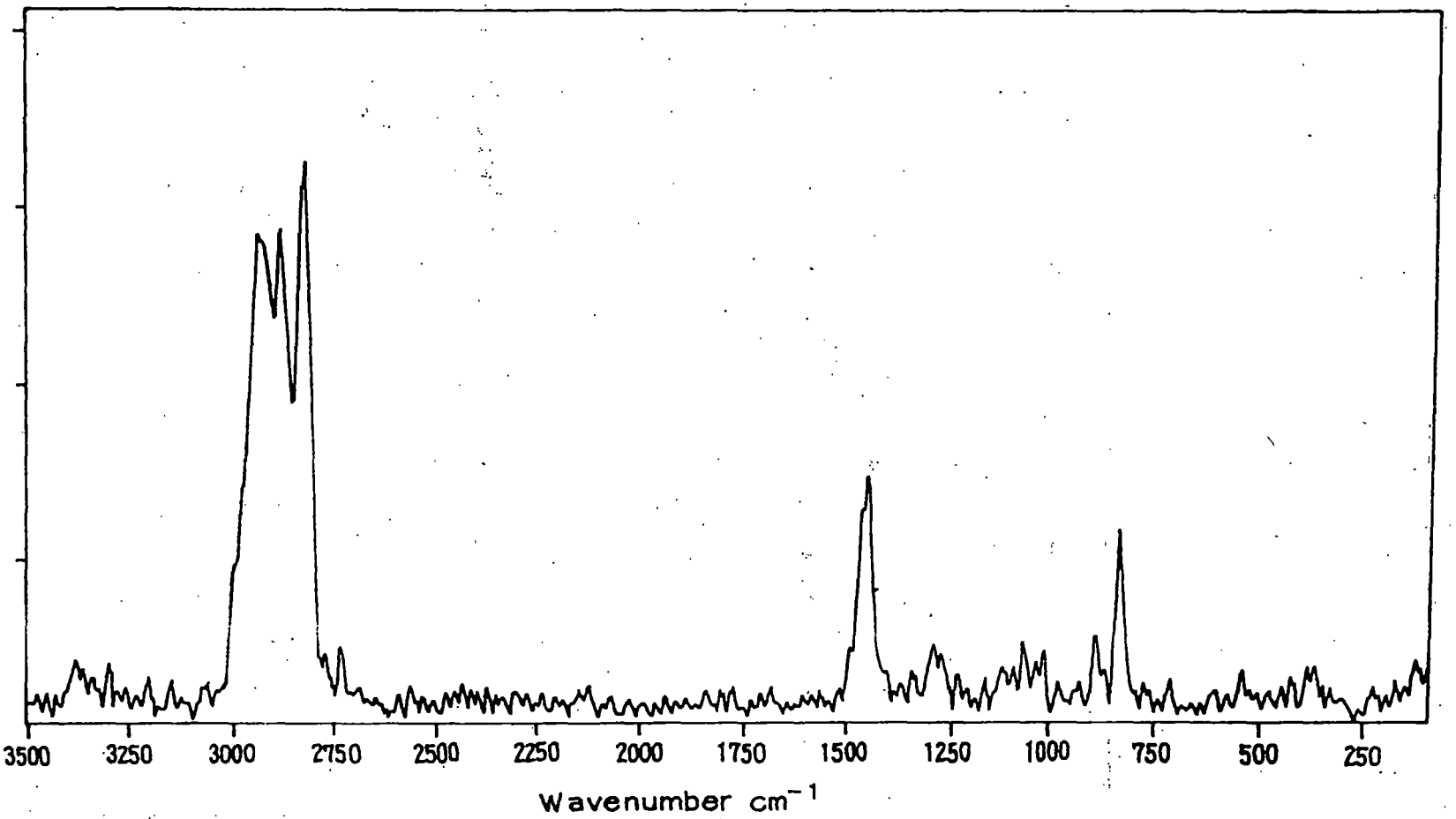

Figure 2: FT-Raman spectrum of Ph_4AsCl in 2-methoxyethanol.

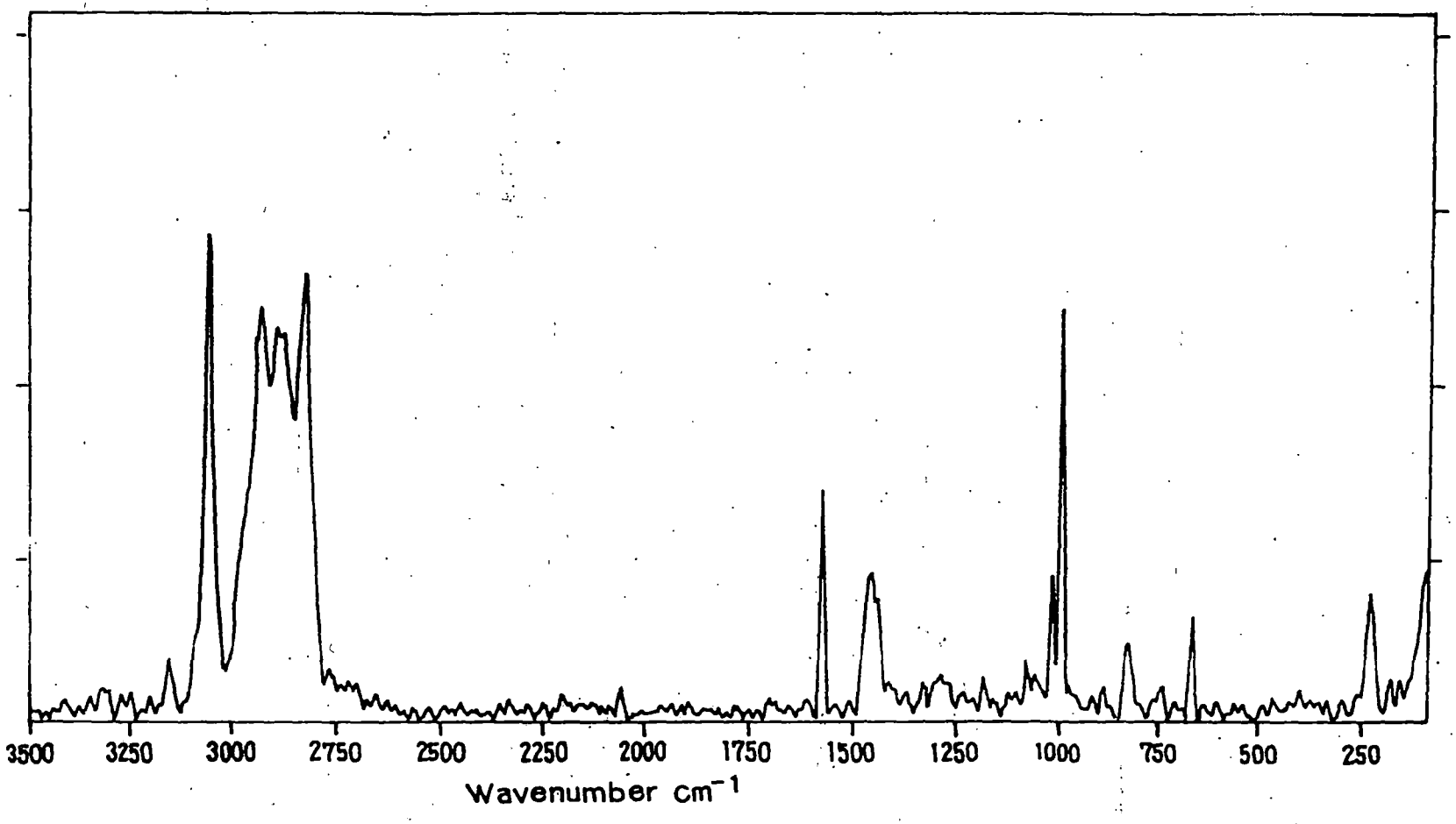

Figure 3: FT-Raman spectrum of Ph_4PBr in 2-methoxyethanol.

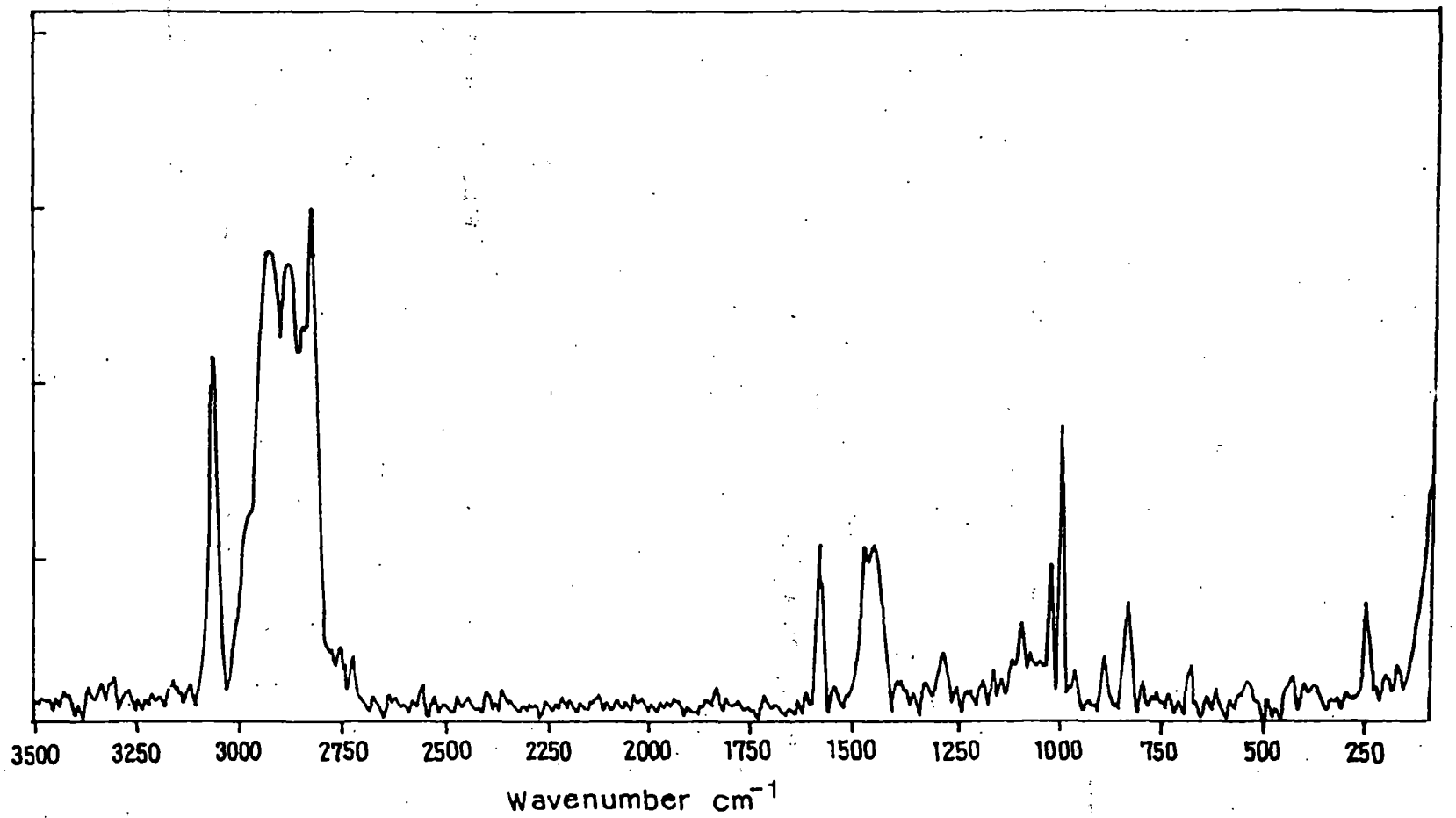

Figure 4: FT-Raman spectrum of $LiBF_4$ in 2-methoxyethanol.

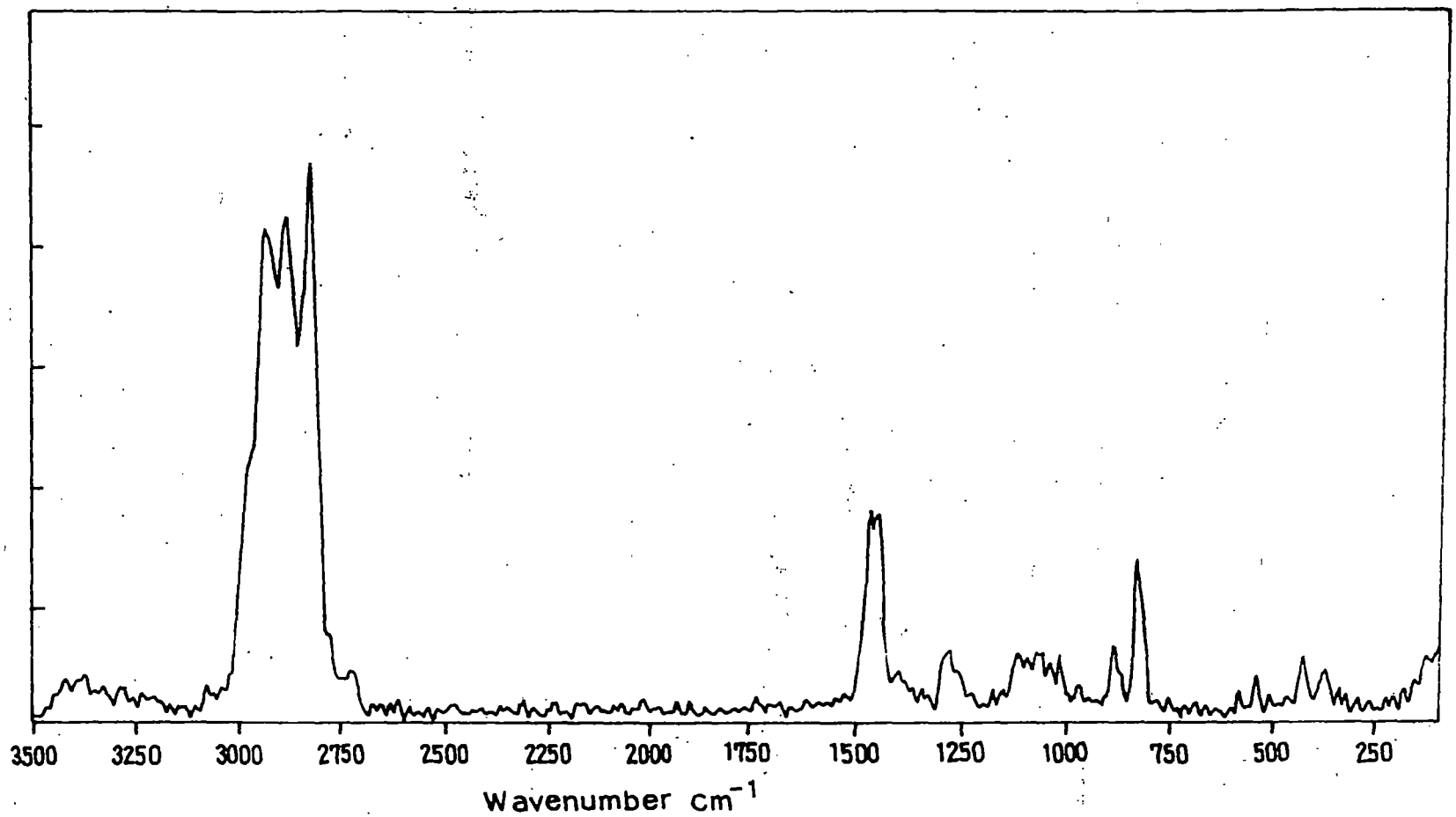

Figure 5: FT-Raman spectrum of $NaBF_4$ in 2-methoxyethanol.